

# Forecasting Related Time Series\*

Ulrich K. Müller and Mark W. Watson

Department of Economics

Princeton University

This Draft: December 19, 2025

## Abstract

A collection of time series are “related” if they follow similar stochastic processes and/or they are statistically dependent. This paper proposes a Related Time Series (RTS) forecasting model that exploits these relationships. The model’s foundation is a set of univariate Gaussian autoregressions, one for each series, which are then augmented to incorporate stochastic volatility, heavy-tailed innovations, additive outliers, time-varying parameters and common factors. The model is estimated and forecasts are computed using Bayesian methods with hierarchical priors that pool information across series. Computationally efficient MCMC methods are proposed. The RTS model is applied to three datasets and yields encouraging pseudo-out-of-sample forecasting results.

Keywords: Bayesian Forecasting, Factor Models, Hierarchical Priors

JEL: C11, C32, C53

---

\*This paper was presented at the 13th Annual International Association of Applied Econometrics Conference in June 2025 as the *Journal of Applied Econometrics* Invited Paper. We thank the organizers for inviting us to write this paper and our discussants James Mitchell and Jonathan Wright for insightful comments.

# 1 Introduction

This paper considers “related” economic time series, where the series may be related in two distinct ways: They may be related because they follow similar stochastic processes and/or because they are statistically dependent. Series generated by autoregressive models with similar autoregressive (AR) coefficients are related in the first way, while variables that interact in a vector autoregression are related in the second way. In either case, information from one series may help forecast the value of another related series, where in the first instance this information involves the values of parameters used for forecasting, and in the second it exploits potential lead/lag relationships between the variables. This paper develops a forecasting model for related time series that utilizes both of these sources of information.

An empirical example used in the sections below helps set the stage. It uses a dataset comprised of monthly employment growth rates in each of the 50 U.S. states and the District of Columbia. While each state is different, they share many common features such as similar serial correlation patterns and variability. Moreover, macroeconomic forces in the U.S. affect all of the states, where these effects are stronger and/or materialize more quickly in some states than others, leading to dynamic cross-correlations among the series. Interest lies in forecasting the states’ employment growth rates over the next several months.

This paper has three related goals. The first is to develop a flexible but tractable model that captures common features and comovement in the series and exploits these relationships for short-term forecasting. For lack of a better name, we call this the “Related Time Series” (RTS) model. The paper’s second goal is to develop a set of numerical algorithms to reliably and efficiently carry out estimation and prediction for the RTS model. The third goal is to evaluate the forecasting performance of the RTS model using the state employment dataset and two unrelated datasets.

We construct the RTS model from familiar ingredients. At its foundation is a collection of univariate Gaussian autoregressions, one for each series. It starts there because univariate AR models provide competitive point forecasts for a wide range of economic variables. Moving beyond point forecasts requires modeling higher-order moments, and the RTS model does this via stochastic volatility, heavy-tailed innovations, and additive outliers. Dependence across series is introduced through commonalities in stochastic volatility realizations and through a set of common factors that capture low-frequency, higher-frequency, and occasional large and irregular comovements in the series. Parameters describing these features are allowed to

slowly evolve through time, so that effectively, the model puts more weight on more recent data when constructing the forecast distribution. The RTS model is estimated using Bayesian methods, where hierarchical priors are used to pool information across series, and we develop a MCMC sampler to approximate posterior distributions.

Our analysis borrows from a vast literature. While it is impossible to do justice to all of the important contributions, we mention a few here. Perhaps the best place to start is with the practical univariate methods described in Box and Jenkins (1970), and the incorporation of innovation and additive outliers in Fox (1972) and Abraham and Box (1979). The stochastic volatility in the RTS model has its genesis in Engle (1982) and the formulation we use builds on Kim, Shephard, and Chib (1998) and Omori, Chib, Shephard, and Nakajima (2007). The RTS model incorporates many features from unobserved component models with classic contributions in Nerlove, Grether, and Carvalho (1979) and Harvey (1989), and the work on factor model forecasting surveyed in Stock and Watson (2016b), related large- $n$  forecasting methods in Banbura, Giannone, and Reichlin (2010), D’Agostino and Giannone (2012), Carriero, Clark, and Marcellino (2015), De Mol, Giannone, and Reichlin (in press) and multi-country VAR models of Chudik and Pesaran (2016), Bai, Carriero, Clark, and Marcellino (2022) and elsewhere. Several researchers have included many of the ingredients present in the RTS model: notable examples include Cogley and Sargent (2005), del Negro and Otrok (2008), Stock and Watson (2016a), Almuzara and Sbordone (2022), Antolin-Diaz, Drechsel, and Petrella (2024), and Carriero, Clark, Marcellino, and Mertens (2024). Gelman, Carlin, Stern, and Rubin (2004) provides a textbook overview of the Bayesian methods that we employ, and these are augmented with insights from Doan, Litterman, and Sims (1984), Meng and Wong (1996), Durbin and Koopman (2002), Geweke (2004), and Chan and Jeliazkov (2009).

The paper is organized as follows. Section 2 introduces the state employment dataset, and documents features of these data (similar autoregressive dynamics, stochastic volatility, outliers, comovement, etc.) that are incorporated in the RTS model. This section also outlines a pseudo-out-of-sample forecasting experiment and the loss functions we use to evaluate the RTS model’s point, quantile and interval forecasts.

Section 3 develops the RTS model and is the heart of the paper. The RTS model includes autoregressive dynamics, heavy-tailed innovations and additive outliers (both modeled as Student- $t$  random variables), low-frequency stochastic volatility with a component that is common across series, time-varying level, autoregressive, and other parameters (modeled

as random walks), and dynamic common factors. The model is estimated and predictions are formed using Bayesian methods, where hierarchical priors are used to pool information across the series. While each of these ingredients is straightforward, taken together they yield a notationally complex RTS model. With this in mind, Section 3 develops the RTS model sequentially: It begins with simple univariate AR models for each series, and then adds ingredients one at a time. This results in seven models, each more complex than its predecessor, and where the final model is the full RTS model.

Section 3 also evaluates the fit and forecasting performance of the model using the state employment data. The results are encouraging. Over the pseudo-out-of-sample period from 2000-2019, the root mean square forecasting error from the RTS model is roughly 10 percent lower than a benchmark AR(12) model,<sup>1</sup> these gains are widespread across the states, and similar gains are obtained for quantile and interval forecasts.

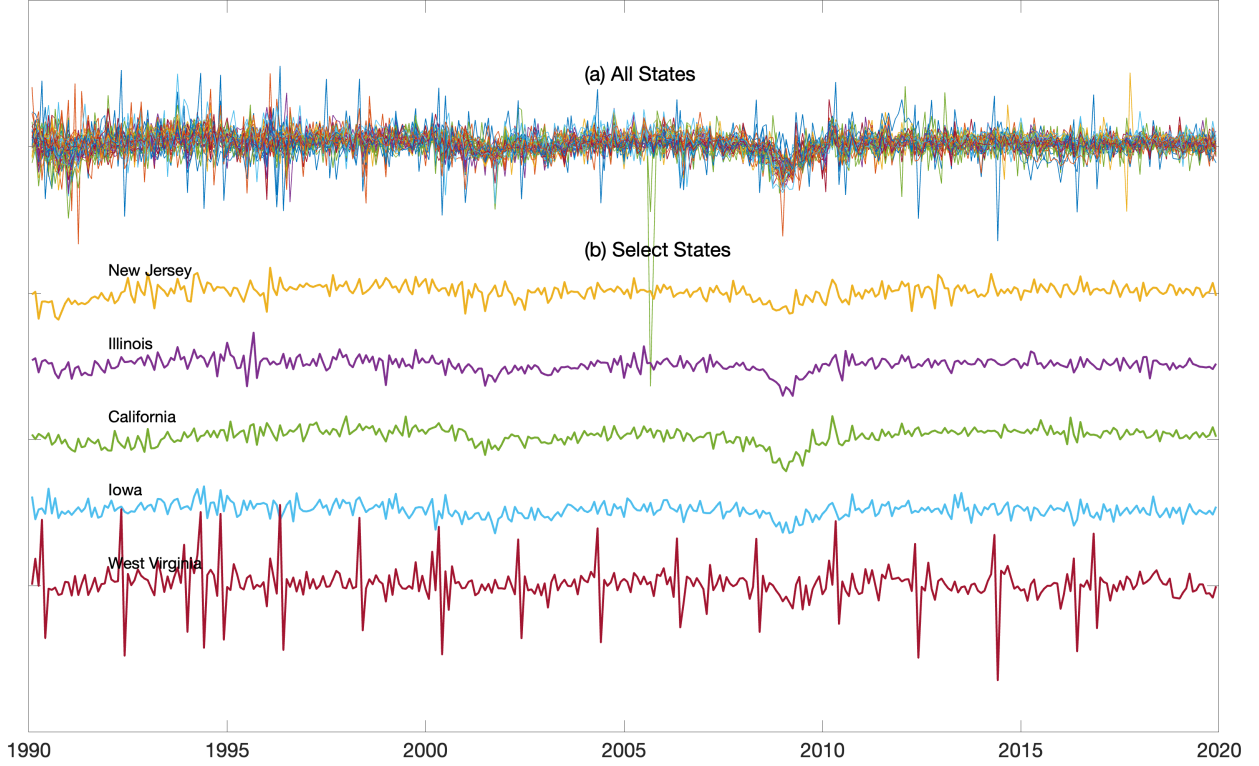
Section 4 summarizes additional empirical exercises that serve as external validity checks for the usefulness of the RTS model. The structure of these exercises is simple. We introduce two new datasets—growth rates of industrial production from 16 Euro-area countries and inflation from 17 sectors making up personal consumption expenditures in the United States—and use the RTS model developed in Section 3, without any modification in the model or prior, in pseudo-out-of-sample forecasting experiments in these datasets. We also examine the forecasting performance of the model during the aftermath of the COVID recession. In each of these exercises, the RTS model performs well.

Section 5 provides concluding remarks, but much of the important work in the paper comes after these remarks: The Online Appendix provides a detailed description of the algorithms used to estimate the model. This discussion parallels the sequential development of the RTS model in Section 3 and highlights, in modular fashion, the features of the algorithm needed to accommodate the various ingredients in the RTS model. Interested users can mix and match these modules when building models that incorporate these ingredients.

---

<sup>1</sup>A 10% decrease of root-MSFE corresponds to having access to a variable whose correlation with the baseline forecast error is equal to 0.44 ( $= \sqrt{1 - 0.9^2}$ ).

Figure 1: Monthly Growth Rates for U.S. States, 1990-2019



Notes: Panel (a) plots the monthly growth rates for employment in each of the 50 U.S. states and the District of Columbia. Panel (b) shows the growth rates for five selected states.

## 2 An initial look at the U.S. States Employment data and a benchmark model

### 2.1 Some Descriptive Statistics

Figure 1 plots seasonally adjusted monthly rates of growth for employment in  $n = 51$  U.S. states and the District of Columbia (hereafter “states”). The sample starts in February 1990 and is plotted through the end of 2019, where for much of our analysis we truncate the sample in 2019m12 to avoid the COVID-19 pandemic and its aftermath. (Section 4.2 presents selected results for the post-2019 period.) Panel (a) plots all 51 series and panel (b) plots the growth rates for a handful of states.<sup>2</sup>

The figure highlights five features of the data that play a role in the RTS forecasting

---

<sup>2</sup>The Online Appendix includes sources and descriptions for the data used in this paper.

Table 1: Selected Statistics for U.S. States Employment Growth Rates

	Quantile				
	0.10	0.25	0.50	0.75	0.90
<i>(a) AR(12) Model</i>					
Sum of AR Coefficients	0.49	0.60	0.69	0.73	0.81
Innovation Standard Deviation	2.18	2.42	2.89	3.42	4.44
<i>(b) GARCH(1,1) Student-t Model</i>					
Sum of GARCH Coefficient	0.25	0.47	0.73	0.93	0.98
Student-t degrees of freedom	4.2	5.4	6.3	7.7	13.8
<i>(c) p-values for Nyblom test statistics</i>					
Level	< 0.01	0.04	0.30	0.51	0.67
Sum of AR Coefficients	0.02	0.23	0.56	0.78	0.90

Notes: The columns show the quantiles of the distribution of row-statistics across the 51 states.

model. We discuss these in turn.

First, the growth rates are correlated across states. For example, the figure shows that the 2007-2009 recession led to synchronized declines in employment across the U.S. states, and the 1990-1991 and 2001 recessions also led to widespread, but less severe, declines. The average pairwise correlation of year-over-year growth rates was 0.33 over the 1990-2019 sample period.

Second, the series have similar second moment properties. For example, consider the following state-specific univariate AR(12) models:

$$\phi_i(L)(y_{i,t} - \mu_i) = \varepsilon_{i,t}. \quad (1)$$

Panel (a) of Table 1 shows the distribution (across states) of the sum of the OLS-estimated AR coefficients,  $\hat{\phi}_i(1)$ , and the residual standard deviation,  $\hat{\sigma}_{\varepsilon_i}$ . They indicate similar patterns of long-run persistence and variability for many of the states. An examination of the AR filter gains,  $|\hat{\phi}_i(e^{i\omega})|$ , also indicates a similar pattern of persistence across all frequencies. (The gains are not shown to conserve space).

Third, there are obvious outliers in the employment data. The largest outlier in Figure 1 is associated with Hurricane Katrina in August 2005 which caused large employment losses in Louisiana. Several outliers are also evident in the data for West Virginia plotted in panel (b), where many of these employment changes are associated with mining employment.

Fourth, time-varying volatility in growth rates is also evident. One simple way to gauge the prevalence of volatility shifts is by examining estimated parameters from GARCH(1,1) models

for the innovations in the AR(12) models in (1). The distribution (across states) for the sum of these GARCH coefficients is shown in panel (b) of Table 1, and indicates persistent changes in volatility for most states. The estimated GARCH models include Student- $t$  innovations, and the table also shows the distribution of the estimated degrees of freedom; these are small, capturing the outliers and kurtosis in the innovations.

Fifth, but more difficult to see in the figure, is time variation in the levels of the growth rates—that is, time variation of  $\mu_i$  in (1). Also of interest is potential time variation in the AR coefficients in  $\phi_i(L)$ . Panel (c) of Table 1 shows the distribution of the  $p$ -value of Nyblom (1989) tests for the null of constancy versus the alternative of random walk variation in these coefficients. The  $p$ -values suggest time variation in the level parameter for many of the states, but provide little evidence of time variation in the AR coefficients.

The RTS forecasting model, developed in Section 3, is designed to capture these five features of the data. Before presenting the model, we outline the pseudo-out-of-sample (POOS) forecasting experiment used to evaluate its performance.

## 2.2 Recursive pseudo-out-of-sample forecasting and criteria for forecast evaluation

### 2.2.1 Description of experiment

The AR(12) model in (1) will serve as a convenient benchmark for the forecasts, and we use that model to describe the recursive pseudo-out-of-sample (POOS) forecasting experiment. The experiment proceeds in the usual way. The full sample ranges from  $t = 1, \dots, T$  (where in this application  $t = 1$  is 1990m2 and  $T$  is 2019m12). Let  $\text{Emp}_{i,t}$  denote the level of employment in state  $i$  in month  $t$ , and let  $y_{i,t} = 1200 \times \ln(\text{Emp}_{i,t} / \text{Emp}_{i,t-1})$  denote the monthly growth rates plotted in Figure 1, measured in percentage points at an annual rate. Let  $y_{i,t+h}^h = (1200/h) \times \ln(\text{Emp}_{i,t+h} / \text{Emp}_{i,t})$  denote the growth rate from  $t$  to  $t + h$ , again measured in annual percentage points. The goal is to forecast the values of  $y_{i,t+h}^h$  for  $h = 1, 3, 6$  months ahead. Forecasts are computed recursively: Using data from  $t = 1, \dots, T^*$  with  $T^* = T_1$ , the model parameters are estimated and forecasts (point, quantile and interval) are computed for  $y_{i,T^*+h}^h$ . This process is repeated for  $T^* = T_1 + 1, T_1 + 2, \dots, T - h$ . The forecasting experiment is carried out using the data plotted in Figure 1, which are the currently available historical data and not “real time” data; state-level employment data undergo significant revisions and our analysis abstracts from these revisions. In the application the POOS experiment begins

in  $T_1 = 1999m12$ , so that the first POOS forecast is based on ten years of in-sample data.<sup>3</sup>

### 2.2.2 Forecast Loss Function

We are interested in point forecasts, predictive quantiles and interval forecasts. Let  $y$  denote the random variable of interest,  $\hat{y}$  denote the point forecast,  $q_\alpha$  denote the  $\alpha$ th quantile of the predictive distribution of  $y$  with  $\hat{q}_\alpha$  its estimate,  $(q_{\alpha/2}, q_{(1-\alpha/2)})$  denote the equal-tailed  $1 - \alpha$  prediction interval and  $(\hat{q}_{\alpha/2}, \hat{q}_{(1-\alpha/2)})$  denote its estimate. We evaluate the forecasts using standard loss functions:

- Squared error loss for point forecasts:  $\ell(y, \hat{y}) = (y - \hat{y})^2$  with resulting mean squared forecast error (MSFE) as the expected loss. We will report root-MSFEs.
- Quantile loss:  $\ell(y, \hat{q}_\alpha) = \begin{cases} \alpha(y - \hat{q}_\alpha) & \text{for } y \geq \hat{q}_\alpha \\ (1 - \alpha)(\hat{q}_\alpha - y) & \text{for } y < \hat{q}_\alpha \end{cases}$ .
- Interval loss:

$$\ell(y, \hat{q}_{\alpha/2}, \hat{q}_{(1-\alpha/2)}) = (\hat{q}_{(1-\alpha/2)} - \hat{q}_{\alpha/2}) + \frac{2}{\alpha} ((\hat{q}_{\alpha/2} - y) \times \mathbf{1}[y < \hat{q}_{\alpha/2}] + (y - \hat{q}_{(1-\alpha/2)}) \times \mathbf{1}[y > \hat{q}_{(1-\alpha/2)}]).$$

As is well-known, the risks associated with these losses are minimized using the mean of the predictive distribution for  $\hat{y}$ ,  $\hat{q}_\alpha = q_\alpha$  and  $(\hat{q}_{\alpha/2}, \hat{q}_{(1-\alpha/2)}) = (q_{\alpha/2}, q_{(1-\alpha/2)})$ .

We compute sample average values of these losses (i.e., sample risk) for each of the forecasting models and forecast horizons.

## 3 Seven models

This section is the heart of the paper. Here we develop a tractable forecasting model for “related time series” that exhibit the features—similar dynamics, time-varying volatility, co-movement, etc.—that are evident in the state employment data. The model that accommodates all of these features turns out to be rather complex and to understand its various

---

<sup>3</sup>Our interest is in forecasting the growth rates for each of the individual states. In principle, these forecasts could be aggregated to produce a forecast for the growth rate of national employment, although, in the United States, the national and state-level employment data are constructed from different surveys (the CES and CES-SA, respectively), and the state-level employment values do not sum to the national values. There is a large literature on forecasting aggregate series using disaggregates. See Hendry and Hubrich (2011) for discussion and references.

ingredients and the associated computational methods for constructing forecasts, we find it useful to begin with the benchmark AR(12) model in (1) and sequentially add the ingredients. This results in a sequence of seven increasingly rich forecasting models that culminate in the RTS model. The Online Appendix provides a detailed description of computational algorithms for estimating these models, where the increasing complexity of the algorithms allows us to highlight, in a modular way, the necessary modifications required for each model’s new features.

The AR(12) model (1), estimated by OLS and with Gaussian i.i.d. errors, will serve as the benchmark in the POOS forecast comparisons. The first of the seven models we consider is this univariate AR(12) model, but estimated by Bayesian methods using standard “Minnesota” priors. In this model, each of the series is modeled in isolation and any relationships between the series are ignored. The second model is similar to the first, but recognizes that the series are potentially related by having similar parameter values; it exploits this similarity through the use of hierarchical priors. The third model builds on the second, but replaces the Gaussian assumption for the innovations with Student- $t$  distributions with series-specific degrees of freedom, where again hierarchical priors are used to exploit potential similarity of the degrees-of-freedom parameter. This model allows for heavy-tailed innovation outliers that induce dynamic effects on the series through the model’s AR dynamics. The fourth model adds additive outliers, also modeled as Student- $t$  distributed random variables, that induce one-off outliers in the series. The fifth model incorporates stochastic volatility, using a low-frequency formulation that captures both idiosyncratic and common volatility shifts. The sixth model allows for time variation in the level and autoregressive parameters. Each of these models is a version of the univariate AR model so that, conditional on the parameter values, the conditional first moments of the series evolve independently; in these models the series’ conditional first moments are “related” only because they (potentially) have similar parameter values, and this relationship is incorporated through the use of hierarchical priors. The final model is the RTS model that additionally includes comovement in the series by incorporating common latent factors; in this model, employment growth in some states might lead other states and improve the forecasts.

We use the following notation to describe the models. We write  $x_t \sim RW(x_1, \gamma^2)$  to describe a Gaussian random walk with initial value  $x_1$  and innovation variance  $\gamma^2$ . With  $x_t$  a scalar, the vector  $(x_t, x_{t+1}, \dots, x_{t+k})'$  is denoted by  $x_{t:t+k}$ . For a random variable  $x$ , we denote its mean and variance by  $m_x$  and  $v_x$ . Hierarchical priors play an important role in the models,

and throughout we will use a Gaussian hierarchical distribution of the following form: Let  $\{\theta_j\}_{j=1}^n$  denote  $n$  random variables with

$$\theta_j | (m_\theta, v_\theta) \sim iid \mathcal{N}(m_\theta, v_\theta)$$

where  $m_\theta$  and  $v_\theta$  are independent with

$$m_\theta \sim \mathcal{N}(m_{m_\theta}, v_{m_\theta}), \quad \ln(v_\theta) \sim \mathcal{N}(m_{\ln(v_\theta)}, v_{\ln(v_\theta)}).$$

We write this as

$$\{\theta_j\}_{j=1}^n \sim \mathcal{HN}(m_{m_\theta}, v_{m_\theta}, m_{\ln(v_\theta)}, v_{\ln(v_\theta)}). \quad (2)$$

The six precursor models and the final RTS model are presented in the following seven sub-sections. These sections also evaluate the forecasting performance of the models using the POOS forecasting experiment and the state employment dataset. The change in forecast accuracy associated with each model provides a measure of the importance of that model's new feature, albeit in a way that depends on the order in which the features are added to the benchmark model. Ultimately, the forecasting performance of the final RTS model, which includes all of the features, is the object of interest. Section 3.8 complements these forecast comparisons with Bayes factors to evaluate the marginal importance of various features incorporated in the RTS model.

To facilitate the discussion of each model's forecasting performance, Tables 2 and 3 and Figure 2 summarize the results of the various POOS forecasting experiments. As described above, in these experiments, data from 1990m2 ( $t = 1$ ) through  $t = T^*$  is used to construct forecasts for time periods  $T^* + h$ , where in this exercise,  $T^*$  ranges from 1999m12 through 2019m6 and  $h = 1, 3$ , and 6. Table 2 shows the root mean square forecast error (root-MSFE) for each of the methods, where forecast errors results are pooled across the 51 states. The first panel of this table shows the root-MSFE for the benchmark AR(12) model and the values in panel (b) show the values of the root-MSFE for each of the methods relative to the benchmark model.<sup>4</sup> Figure 2 uses box plots to summarize the distribution of these relative

---

<sup>4</sup>We also computed a version of Table 2 that attenuated the effect of outliers evident in Figure 1. Specifically, when computing the forecast errors used for the root mean square forecast error we replaced realizations of  $y_{i,t}$  that deviated from the sample median by more than four times the interquartile range with the local median of  $y_{i,t^*}$  for  $t^* \in (t - 3, t + 3)$ . The resulting relative root-MSFEs for Models I-VII were similar to, but somewhat smaller than the values shown in Table 2. For example, the values for the RTS model (Model VII) were (0.90, 0.88, 0.89) for  $h = 1, 3, 6$ .

root-MSFEs across the 51 states. Table 3 shows the sample risk values for the predictive quantiles and the 80 percent (90-10) equal-tailed prediction intervals, where the values are relative to the benchmark AR(12) model and are pooled across states. We discuss these results in the following subsections, but for now we simply note that the results show progressively more accurate point, quantile and interval forecasts as features are added to the model. In particular, the final RTS model yields a root-MSFE that is 8-11% lower than the benchmark model and shows similar gains for the quantile and interval forecasts.

Table 2: Root Mean Square Forecast Errors (Pooled Across States)

Forecasting Model	Forecast of Employment Growth Rate from $T$ to $T+h$		
	$h = 1$	$h = 3$	$h = 6$
	(a) Root MSFE (percentage points at an annual rate)		
Benchmark AR(12)	3.3	2.1	1.8
	(a) Relative Root MSFE		
Benchmark AR(12)	1.00	1.00	1.00
I: Bayes Shrinkage	0.98	1.00	1.02
II: Hier. Priors	0.96	0.95	0.96
III: Innov. Outliers	0.96	0.95	0.96
IV: Add. Outliers	0.96	0.95	0.96
V: Stoch. Vol.	0.96	0.95	0.95
VI: TVP	0.95	0.94	0.96
VII: RTS Model	0.92	0.89	0.89

Notes: Pseudo-out-of-sample forecasting root mean square forecast errors for the benchmark AR(12) and seven forecasting models discussed in Sections 3.1-3.7.

### 3.1 Model I: Bayesian shrinkage

The first model is the univariate AR(12) that utilizes independent (and standard) priors for the model's parameters. We present the model using different notation than we used in (1) as this facilitates the presentation of Models II-VII. In particular, we write Model I as

$$y_{j,t} = \mu_j + \omega u_{j,t} \quad (3)$$

$$u_{j,t} = \sum_{l=1}^p \phi_{j,l} u_{j,t-l} + \epsilon_{j,t} \quad (4)$$

$$\epsilon_{j,t} = \sigma_j \varepsilon_{j,t} \quad (5)$$

$$\varepsilon_{j,t} \sim iid\mathcal{N}(0, 1) \quad (6)$$

Table 3: Relative Values of Sample Quantile and Interval Risk (Pooled Across States)

Model	Quantile						90-10 Interval
	0.05	0.10	0.25	0.75	0.90	0.95	
(a) $h = 1$							
Benchmark	1.00	1.00	1.00	1.00	1.00	1.00	1.00
I: Bayes Shrinkage	1.00	1.00	0.99	0.99	1.00	0.99	1.00
II: Hier. Priors	0.98	0.98	0.97	0.97	0.98	0.98	0.98
III: Innov. Outliers	0.97	0.96	0.95	0.93	0.94	0.96	0.95
IV: Add. Outliers	0.97	0.96	0.95	0.93	0.94	0.96	0.95
V: Stoch. Vol.	0.96	0.96	0.95	0.92	0.91	0.92	0.93
VI: TVP	0.95	0.95	0.94	0.92	0.91	0.91	0.93
VII: RTS Model	0.92	0.92	0.92	0.89	0.89	0.89	0.90
(b) $h = 3$							
Benchmark	1.00	1.00	1.00	1.00	1.00	1.00	1.00
I: Bayes Shrinkage	1.04	1.04	1.03	1.00	1.00	0.99	1.02
II: Hier. Priors	0.94	0.95	0.96	0.97	0.97	0.97	0.96
III: Innov. Outliers	0.92	0.94	0.95	0.95	0.96	0.97	0.95
IV: Add. Outliers	0.92	0.94	0.95	0.95	0.96	0.97	0.95
V: Stoch. Vol.	0.92	0.93	0.94	0.93	0.91	0.91	0.92
VI: TVP	0.88	0.9	0.94	0.95	0.93	0.93	0.92
VII: RTS Model	0.83	0.85	0.88	0.91	0.89	0.87	0.87
(c) $h = 6$							
Benchmark	1.00	1.00	1.00	1.00	1.00	1.00	1.00
I: Bayes Shrinkage	1.08	1.08	1.06	0.97	0.96	0.94	1.03
II: Hier. Priors	0.90	0.94	0.96	0.97	0.96	0.94	0.95
III: Innov. Outliers	0.88	0.92	0.95	0.97	0.97	0.96	0.94
IV: Add. Outliers	0.88	0.92	0.95	0.97	0.97	0.96	0.94
V: Stoch. Vol.	0.90	0.92	0.94	0.93	0.9	0.88	0.91
VI: TVP	0.83	0.88	0.94	0.99	0.99	0.98	0.92
VII: RTS Model	0.79	0.83	0.88	0.92	0.89	0.87	0.86

Notes: Pseudo-out-of-sample sample average losses relative to the benchmark AR(12) for the seven forecasting models discussed in Sections 3.1-3.7.

where the number of lags in the AR model (4) is  $p = 12$ . Note that the model introduces a common scale parameter  $\omega$ , so the parameters  $\sigma_j$  capture the relative volatilities of the series. The level of each series is given by  $\mu_j$ .

The model is estimated using the following priors:

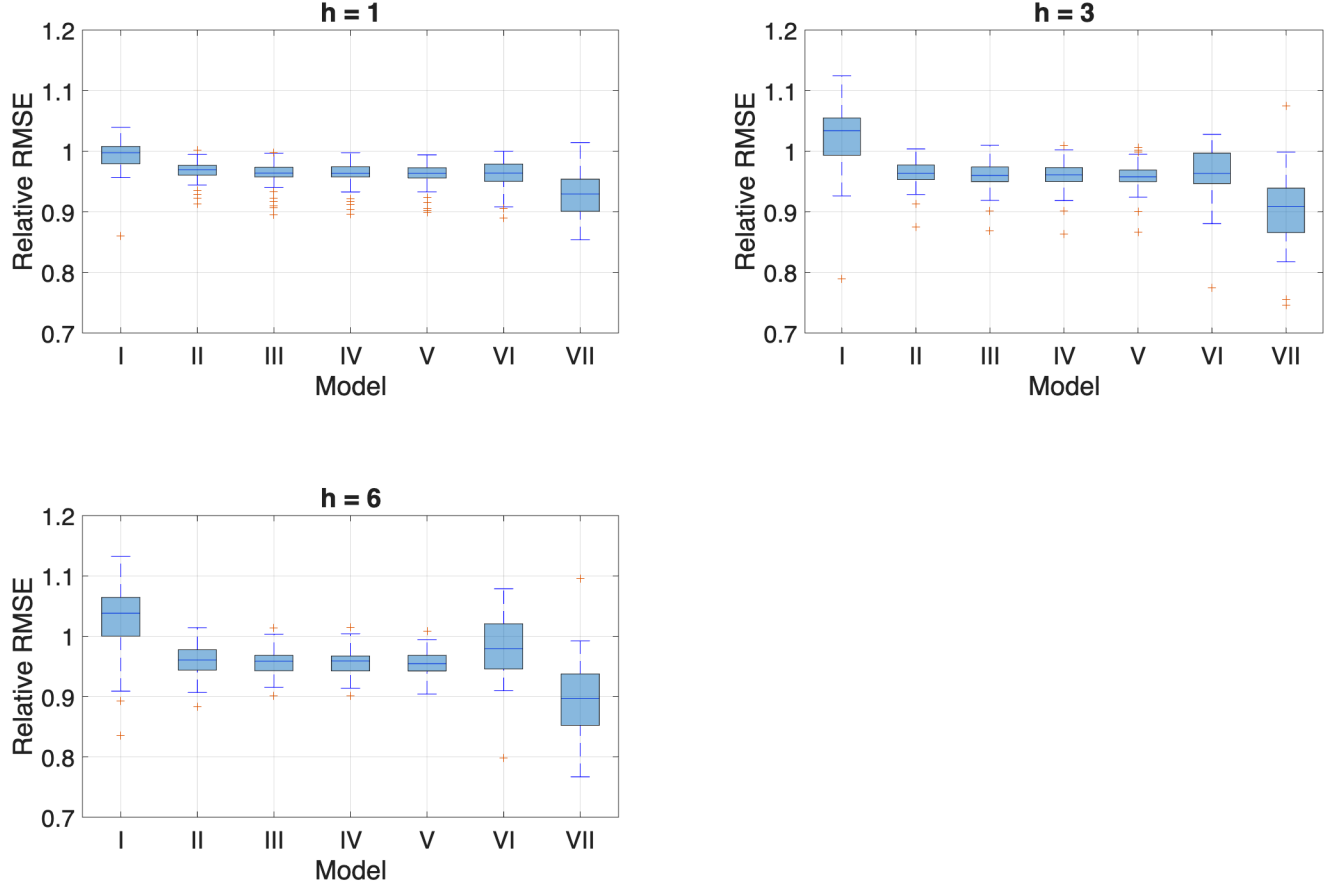
- To induce scale and location equivariance, the priors for  $\omega$  and  $\{\mu_j\}_{j=1}^n$  are diffuse:

$$\ln(\omega^2) \sim \mathcal{N}(0, \infty) \quad (7)$$

and

$$\mu_j \sim \mathcal{N}(0, \infty). \quad (8)$$

Figure 2: Relative Root Mean Forecast Error Distribution Across States



Notes: Box plots for the relative root-MSFEs for the 51 states. The models are discussed in Sections 3.1-3.7, where Model VII is the RTS model.

- The model requires values for the initial values  $\{u_{j,t}\}_{t=-11}^0$ , and we assume that these are draws from a stationary AR model. Specifically, with  $\phi_j = \{\phi_{j,l}\}_{l=1}^{12}$ , the prior for  $\{u_{j,t}\}_{t=-11}^0$  is

$$u_{j,-11:0} | (\sigma_j, \phi_j) \sim \mathcal{N}(0, \sigma_j^2 \Sigma(\phi_j)) \text{ with } \Sigma(\phi) = \Sigma_{AR}(c\phi) \quad (9)$$

where  $\Sigma_{AR}(\phi)$  is the  $p \times p$  covariance matrix of the stationary  $\text{AR}(p)$  model with AR coefficient vector  $\phi$  and unit innovation variance, and where the constant  $c \leq 1$  in (9) is chosen so that the largest root of the companion matrix is no larger than 0.98. This prior allows the distribution of the initial conditions to depend on the AR parameters  $(\sigma_j, \phi_j)$ , but in a way that bounds the variance when the AR parameters yield explosive

dynamics.

- We use Minnesota-like priors for AR coefficients:

$$\phi_{j,l} \sim \mathcal{N}(0, (0.2/l)^2). \quad (10)$$

The value of 0.2 means the values are strongly shrunk toward zero, increasingly so for longer lags.

- The prior for  $\sigma_j$  is

$$\ln(\sigma_j^2) \sim \mathcal{N}(0, 0.3^2). \quad (11)$$

Recall that  $\omega$  captures the overall scale of the data, with  $\sigma_j$  parameterizing the relative variability for the  $j$ th state. This prior yields a median of 1.0 for  $\sigma_j$  and places approximately 90 percent of its mass on values of  $\sigma_j$  that are between 0.8 and 1.3.

In summary, Model I is given by equations (3)-(6), with priors given by (7)-(11).

The Online Appendix contains a detailed description of the algorithm used to obtain draws from the posterior distribution of the model's parameters. The algorithm contains familiar steps, although these are modified in important ways for the inclusion of the common scale  $\omega$  and the initial conditions  $\{u_{j,t}\}_{t=-11}^0$ . Draws from the predictive distribution use these draws, augmented with draws of  $\varepsilon_{j,t}$  for  $t = T^* + 1, \dots, T^* + h$  using (6), to obtain draws of  $y_{j,T^*+h}^h$ .

The pseudo-out-of-sample forecasting results reported in Tables 2 and 3 and Figure 2 suggest this model's forecast accuracy is roughly on par with the benchmark. Perhaps unsurprisingly, Bayesian forecasts using these priors do not improve on simple OLS-based forecasts since this model ignores any relationship between the time series.

### 3.2 Model II: Hierarchical priors

Model II replaces Model I's priors for the AR coefficients and innovation variances with hierarchical priors. These priors exploit similarities in parameter values across the series, potentially sharpening the accuracy of the parameter estimates and forecasts. Specifically, Model II uses the following prior for  $\phi$ :

$$\{\phi_{j,l}\}_{j=1}^n \sim \mathcal{HN}(0, 0.5^2(0.2/l)^2, \ln((0.2/l)^2), 0.5^2). \quad (12)$$

Unpacking the prior using the notation in (2): (12) says that  $\phi_{j,l}|(m_{\phi_l}, v_{\phi_l}) \sim iid\mathcal{N}(m_{\phi_l}, v_{\phi_l})$ , but with  $m_{\phi_l} \sim \mathcal{N}(0, 0.5^2(0.2/l)^2)$  and  $\ln(v_{\phi_l}) \sim \mathcal{N}(\ln((0.2/l)^2), 0.5^2)$ . The resulting estimates of  $\phi_{j,l}$  are shrunk towards  $m_{\phi_l}$  with a strength governed by  $v_{\phi_l}$ , where the data help inform appropriate values of  $m_{\phi_l}$  and  $v_{\phi_l}$ .

A hierarchical prior is also used for  $\sigma_j$ :

$$\{\ln(\sigma_j^2)\}_{j=1}^n \sim \mathcal{HN}(0, 0.5^2, \ln(0.3^2), 0.5^2) \quad (13)$$

so again, information from all of the series is used to inform the posterior for  $\sigma_j$ .

The estimation algorithm presented in the Online Appendix provides a computationally efficient method for incorporating these hierarchical priors into the analysis.

Tables 2 and 3 and Figure 2 indicate that Model II provides markedly more accurate forecasts than the benchmark AR(12) and its Bayesian implementation in Model I. The root-MSFEs are 4-6 percent smaller than the benchmark across the different horizons (Table 2), the improvement is widespread across the states (Figure 2), and quantile and interval forecasts are improved (Table 3).

Figure 3 provides some insight into this gain. It plots the prior for the AR coefficients from Model I together with the “prior” in Model II,  $\phi_{j,l}|(m_{\phi_l}, v_{\phi_l}) \sim iid\mathcal{N}(m_{\phi_l}, v_{\phi_l})$ , evaluated at the posterior mean of  $m_{\phi_l}$  and  $\ln v_{\phi_l}$  using data through 2019m12. While the prior for Model I shrinks the AR coefficients towards zero (the prior mean), Model II’s hierarchical prior shrinks the coefficients toward non-zero values, particularly for lags two through six. This data-dependent shrinkage results in substantially better forecasts for state employment.

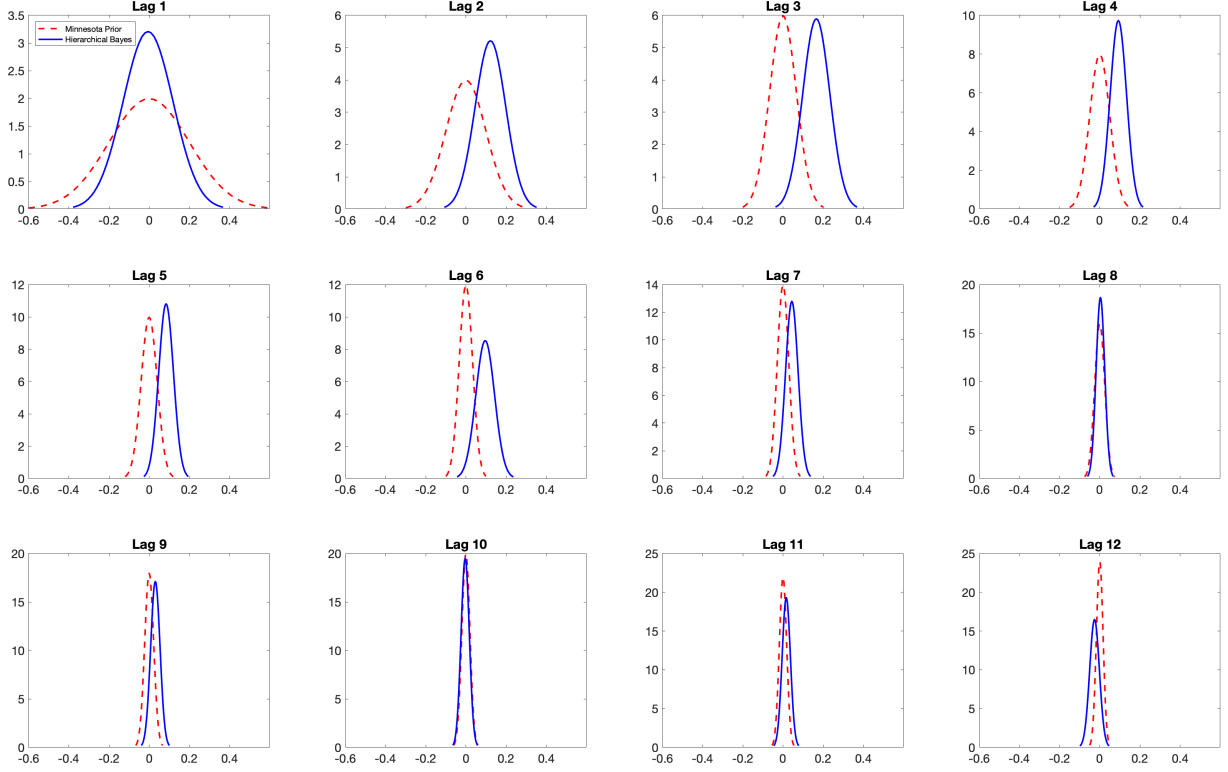
### 3.3 Model III: Student-*t* innovations

In Models I and II, the innovations  $\varepsilon_{j,t}$  are normally distributed, which is at odds with the outliers evident in Figure 1. In Models III and IV, Student-*t* errors are introduced to describe these outliers. In particular, in Model III, the Gaussian assumption (6) is replaced with

$$\varepsilon_{j,t} \sim \mathcal{T}(\nu_j) \quad (14)$$

where  $\mathcal{T}(\nu_j)$  denotes the Student-*t* distribution with  $\nu_j$  degrees of freedom.

Figure 3: Model I's Prior and Model II's Estimated 'Prior'



Notes: For Model I these are the priors in (10). For Model II, this is the normal prior  $\phi_{j,t}|(m_{\phi_t}, v_{\phi_t}) \sim iid\mathcal{N}(m_{\phi_t}, v_{\phi_t})$ , evaluated at the posterior mean of  $m_{\phi_t}$  and  $\ln v_{\phi_t}$  from 2019m12.

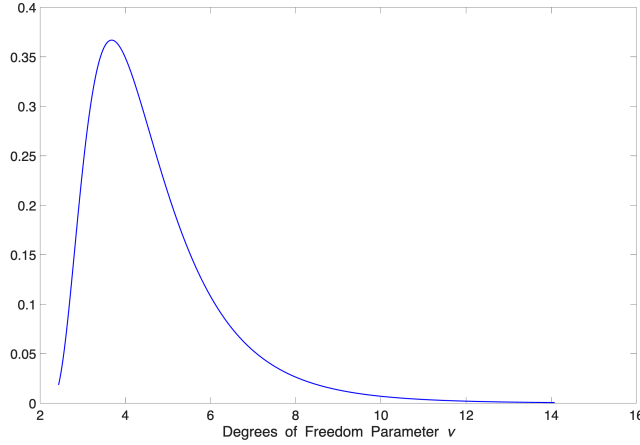
A hierarchical prior is used for the series-specific values of  $\nu_j$ :

$$\{\ln(\nu_j - 2)\}_{j=1}^n \sim \mathcal{HN}(\ln(12 - 2), 0.5^2, \ln(0.5^2), 0.5^2). \quad (15)$$

This prior restricts  $\nu_j$  to be greater than 2, it has a median of 12 and roughly 95 percent of its mass between 4 and 44. Figure 4 plots the prior evaluated at the (2019m12) posterior mean of the hyperparameters; it implies heavy-tailed innovations with degrees of freedom in the range of 3-7, which are broadly consistent with the values shown previously in Table 1.

The Bayes factors that will be presented in Section 3.8 indicate that these heavy-tailed innovations are important for describing the state employment data. In principle, by more accurately modeling the tails of the innovations, they should yield more accurate estimates of the mean parameters,  $\mu$  and  $\phi$ , and therefore produce more accurate point forecasts. The root-MSFE results in Table 2 and Figure 2 suggest that these forecasting gains are small.

Figure 4: Estimated ‘Prior’  $\nu$  in Model III



Note: This is the density of  $\nu$  from  $\ln(\nu_j - 2) | (m_{\ln(\nu-2)}, v_{\ln(\nu-2)}) \sim iid\mathcal{N}(m_{\ln(\nu-1)}, v_{\ln(\nu-2)})$  evaluated at the posterior mean of  $m_{\ln(\nu-2)}$  and  $v_{\ln(\nu-2)}$  from 2019m12.

However, by more accurately modeling the tails, they do improve the quantile and interval forecasts (Table 3).

### 3.4 Model IV: Additive outliers

The heavy-tailed errors in Model III were in the innovations, and therefore produced outliers that propagated forward using the model’s autoregressive dynamics. Model IV introduces new errors that are additive and have one-off effects on the variables. These additive outliers are denoted  $o_{j,t}$  and enter the model with equation (3) replaced by

$$y_{j,t} = \mu_j + \omega(u_{j,t} + o_{j,t}) \quad (16)$$

where

$$o_{j,t} = \kappa_j \eta_{j,t} \text{ and } \eta_{j,t} \sim \mathcal{T}(\nu_j^o). \quad (17)$$

The additive outliers are governed by two parameters:  $\kappa_j$  determines their scale, and the degree-of-freedom parameter  $\nu_j^o$  determines their kurtosis. Hierarchical priors are used for these parameters:

$$\{\ln(\kappa_j^2)\}_{j=1}^n \sim \mathcal{HN}(\ln(0.1^2), 0.5^2, \ln(0.3^2), 0.5^2) \quad (18)$$

$$\{\ln(\nu_j^o - 2)\}_{j=1}^n \sim \mathcal{HN}(\ln(4 - 2), 0.5^2, \ln(0.5^2), 0.5^2), \quad (19)$$

where the prior medians of  $\kappa_j$  and  $\nu_j^o$  are 0.1 and 4, respectively.

As we will see from the Bayes factors reported in Section 3.8, these outliers are important for describing the distribution of the data—an unsurprising result given the handful of large outliers seen in Figure 1. That said, Tables 2 and 3 suggest that they have little effect on the forecasts.

### 3.5 Model V: Time-varying volatility

Model V extends Model IV by incorporating stochastic volatility. Specifically, it replaces (5) with

$$\epsilon_{j,t} = \sigma_{j,t} \varepsilon_{j,t} \quad (20)$$

where  $\ln(\sigma_{j,t})$  evolves as a random walk.

A standard way of including random walk stochastic volatility relies on methods like those pioneered in Kim, Shephard, and Chib (1998). We have found computational gains from using an alternative method that builds on a low-frequency approximation to the random walk; these gains are particularly important when modeling comovement in the volatility paths across the series. To explain the method, it is useful to take a short digression to describe the spectral representation of a random walk.

Consider a generic random walk  $x_t \sim RW(x_1, \gamma^2)$  for  $t = 1, \dots, T$ . The typical representation of the vector  $x_{1:T}$  involves the initial value  $x_1$  and the  $T - 1$  random variables  $\Delta x_t \sim iid\mathcal{N}(0, \gamma^2)$  for  $t = 2, \dots, T$ . This representation, along with a numerical approximation for the distribution of  $\ln(\varepsilon_{j,t}^2)$ , is used in the Kim, Shephard, and Chib (1998) method. We use an alternative representation for  $x_{1:T}$  and an alternative approximation. The details are as follows. Let  $\bar{x}$  denote the sample mean of  $x$  and  $\tilde{x}_t = x_t - \bar{x}$  denote its demeaned value. Write the covariance matrix of  $\tilde{x}_{1:T}$  as  $\gamma^2 \bar{\Sigma}_{RW}$ , where  $\bar{\Sigma}_{RW}$  is the  $T \times T$  covariance matrix of a demeaned random walk with unit innovation variance. Write the spectral decomposition of  $\bar{\Sigma}_{RW}$  as  $\bar{\Sigma}_{RW} = \sum_{l=1}^{T-1} \varphi_l \varphi_l'$  where  $\varphi_l = \lambda_l^{1/2} e_l$  with  $\lambda_l$  the  $l$ th eigenvalue of  $\bar{\Sigma}_{RW}$  and  $e_l$  the corresponding unit-length eigenvector. The vector  $\tilde{x}_{1:T}$  can then be represented as  $\tilde{x}_{1:T} = \sum_{l=1}^{T-1} \varphi_l \xi_l$  where  $\xi_l \sim iid\mathcal{N}(0, \gamma^2)$ . Examination of the matrix  $\bar{\Sigma}_{RW}$  shows that  $e_{l,t} \propto \cos\left(\frac{t-1/2}{T} l \pi\right)$  and, approximately,  $\lambda_l^{1/2} \propto l^{-1}$ , which implies that most of the variance of  $\tilde{x}_t$  is associated with the first few eigenvalues and their associated eigenvectors describe the low-frequency variation in  $\tilde{x}_t$ . This motivates the approximation  $x_t = \bar{x} + \tilde{x}_t \approx \bar{x} + \sum_{l=1}^q \varphi_{l,t} \xi_l$ , where  $\varphi_{l,t}$  is the  $t$ th element of  $\varphi_l$  and the approximation truncates the sum using only

$q \ll T - 1$  terms. This approximation models the low-frequency variation in the random walk, but ignores high-frequency variation; in particular, it captures periodicities longer than  $2T/q$ .

With this background, we model the evolution of  $\ln(\sigma_{j,t}^2)$  using the low-frequency random walk:

$$\ln(\sigma_{j,t}^2) = \ln(\sigma_j^2) + \sum_{l=1}^q \varphi_{l,t} \xi_{j,l} \quad (21)$$

where the sum is truncated at  $q = \lfloor T/36 \rfloor$ , and uses priors

$$\{\xi_{j,l}\}_{j=1}^n | (m_{\xi_l}, v_{\xi}) \sim iid \mathcal{N}(m_{\xi_l}, v_{\xi}) \quad (22)$$

with

$$m_{\xi_l} \sim \mathcal{N}(0, 0.01^2) \quad (23)$$

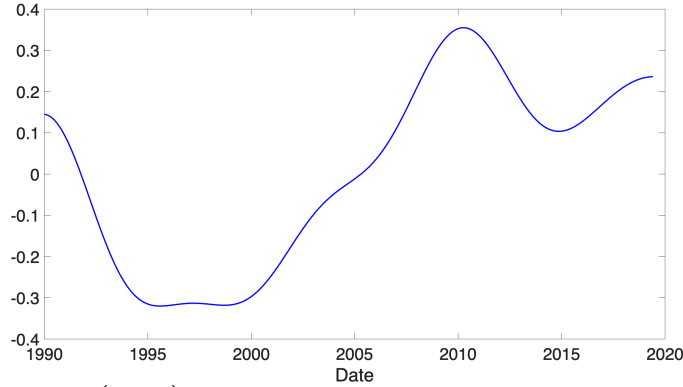
and

$$\ln(v_{\xi}) \sim \mathcal{N}(\ln(0.01^2), 0.5^2). \quad (24)$$

We highlight four features of this specification. First, with  $m_{\xi_l} = 0$  and  $v_{\xi} = \gamma^2$ , (21) is the representation for a random walk that was developed above, truncated after  $q$  terms. Second, the choice of  $q$  means that (21) captures variation in  $\ln(\sigma_{j,t}^2)$  for periods longer than 72 months. Higher-frequency stochastic volatility is not modeled through variation in  $\sigma_{j,t}$  (although it is captured in part through the Student- $t$  errors, which can be represented as scale mixtures of normal random variables). Third, the hierarchical prior allows  $m_{\xi_l}$  to vary across  $l$  in response to the data, capturing comovement in the low-frequency volatility patterns in the series. Figure 5 gives a sense of this common evolution of volatility across the 51 states by plotting  $\sum_{l=1}^q \varphi_{l,t} \hat{m}_{\xi_l}$ , where  $\hat{m}_{\xi_l}$  is the posterior mean of  $m_{\xi_l}$  from 2019m12; it shows a period of relative calm in the late 1990s followed by a marked increase in volatility during the 2007-2009 recession and its aftermath. The fourth feature concerns the role of  $v_{\xi}$  in (21). Notice that, while the mean,  $m_{\xi_l}$ , depends on  $l$ , the variance,  $v_{\xi}$ , does not. Thus  $v_{\xi}$  serves as an overall scale for the variation in  $\ln(\sigma_{j,t})$ , and the posterior for  $v_{\xi}$  summarizes the information in the sample about this scale.

The time variation in  $\ln(\sigma_{j,t})$  introduces an additional step for constructing the predictive distribution of  $y_{j,T^*+h}^h$ , as these are affected by the uncertainty in out-of-sample values of  $\sigma_{j,t}$ .

Figure 5: Estimated Prior Mean for the log-volatility



Notes: The figure plots  $\sum_{l=1}^q \varphi_l \left( \frac{t-1/2}{T} \right) \hat{m}_{\xi_l}$ , where  $\hat{m}_{\xi_l}$  is the posterior mean of  $m_{\xi_l}$  from 2019m12.

Consistent with the random walk model, for  $t > T^*$  we set  $\ln(\sigma_{j,t}) \sim RW(\ln(\sigma_{j,T^*}), v_\xi)$  for independent random walks across  $j$ .

The accuracy of the resulting forecasts is summarized in Tables 2 and 3 and Figure 2. Unsurprisingly, the incorporation of stochastic volatility has little effect on the accuracy of point forecasts (see Table 2 and Figure 2), but significantly improves the accuracy of the predictive quantiles and intervals (Table 3).

### 3.6 Model VI: Time-varying conditional mean parameters

The descriptive statistics reported in Section 2 suggest that the levels of the growth rates,  $\mu_j$  in (16), varied over the sample period in some of the states. There was less evidence of time variation in the autoregressive coefficients,  $\phi_{j,l}$ . In Model VI we allow these coefficients to evolve as random walks, where the amount of time variation is estimated using hierarchical priors.

In particular, Model VI replaces (16) and (4) with

$$y_{j,t} = \mu_{j,t} + \omega(u_{j,t} + o_{j,t}) \quad (25)$$

and

$$u_{j,t} = \sum_{l=1}^p \phi_{j,l,t} u_{j,t-l} + \epsilon_{j,t} \quad (26)$$

where

$$\mu_{j,t} \sim RW(\mu_j, \omega^2 \gamma_{\mu_j}^2) \quad (27)$$

$$\phi_{j,l,t} \sim RW(\phi_{j,l}, \gamma_{\phi_{j,l}}^2). \quad (28)$$

The key parameters governing the evolution of these coefficients are the standard deviations  $\gamma_{\mu_j}$  and  $\gamma_{\phi_{j,l}}$ , which are estimated by pooling information across series using hierarchical priors:

$$\{\ln(\gamma_{\mu_j}^2)\}_{j=1}^n \sim \mathcal{HN}(\ln(0.005^2), 2^2, \ln(0.3^2), 0.5^2) \quad (29)$$

and

$$\{\ln(\gamma_{\phi_{j,l}}^2)\}_{j=1}^n \sim \mathcal{HN}(\ln((0.005/l)^2), 0.5^2, \ln(0.3^2), 0.5^2). \quad (30)$$

The priors for the initial values of the coefficients,  $\mu_j$  and  $\phi_{j,l}$ , are unchanged from the earlier models and are given by (8) and (12). The scaling by  $\omega^2$  in (27) ensures overall location and scale equivariance under the flat priors (8) and (7) on  $\mu_{j,t}$  and  $\omega$ .

Interestingly, while the Bayes factors reported below document the importance of this feature for describing the data, exploiting this time variation for forecasting is difficult. Table 2 indicates that the accuracy of the point estimates, pooled across states, are largely unchanged from Model 5, but Figure 2 shows significantly greater variability in the relative accuracy across states. The relative accuracy of quantile forecasts is also variable showing improvement for some quantiles at some horizons, but deterioration at others.

### 3.7 Common factors and the RTS model

In the models discussed thus far, the series are related through the values of their parameters and, as described in Section 3.5, through dependencies in their stochastic volatility processes. However, conditional on their parameter values, the series are uncorrelated. The RTS model includes common factors to capture covariability in the series. Abstracting from time varying coefficients and stochastic volatility, the introduction of common factors produces a dynamic factor model with autoregressive dynamics for the factor and idiosyncratic errors, which yields a tightly constrained VARMA model. (See Stock and Watson (2016b) for a survey.)

We introduce common factors into the model by replacing (25) with

$$y_{j,t} = \mu_{j,t} + \mu_{n+1,t} + \omega(u_{j,t} + o_{j,t} + o_{n+1,t} + c_{j,t}) \quad (31)$$

where the new ingredients are the factors  $\mu_{n+1,t}$ ,  $o_{n+1,t}$  and  $c_{j,t}$ . There are no observations for  $j = n + 1$ , so these factors are latent. The variable  $\mu_{n+1,t}$  is a common time-varying level that

evolves in the same way as the series-specific level from Model VI, that is as the random walk (27) with  $j = n + 1$ . Similarly, the variable  $o_{n+1,t}$  is a common additive outlier that evolves in the same way as the series-specific outliers in Model IV, that is as (17) with  $j = n + 1$ .

The variable  $c_{j,t}$  is more complicated. It captures potential lead/lag relationships between the series. To explain its evolution, let  $u_{n+1,t}$  evolve the same way as the series-specific values of  $u$ , that is as the AR(12) model (26) for  $j = n + 1$ , with the autoregressive coefficients allowed to vary in time as in (28). The variable  $c_{j,t}$  is a series-specific moving average of  $u_{n+1,t}$ :

$$c_{j,t} = \sum_{l=0}^5 \lambda_{j,l,t} u_{n+1,t-l} \quad (32)$$

where the moving average weights,  $\lambda_{j,l}$  are allowed to vary through time as

$$\lambda_{j,l,t} \sim RW(\lambda_{j,l}, \gamma_{\lambda_{j,l}}^2). \quad (33)$$

In this model, series that load on the first few lags of  $u_{n+1,t}$  serve as leading indicators for series that load on more distant lags, improving the model's forecasts for the lagging series. Moreover, even if all series load only on the contemporaneous value of  $u_{n+1,t}$ , forecasts are potentially improved because the different series provide independent information about  $u_{n+1,t}$ , which in turn follows its own dynamics; the forecasts for the different series are thus effectively shrunk towards a common non-zero value.

The new priors for this model are

$$\ln(\sigma_{n+1}^2) \sim \mathcal{N}(\ln(0.2^2), 0.5^2) \quad (34)$$

$$\mu_{n+1} = 0 \text{ (a normalization), } \ln(\gamma_{\mu_{n+1}}^2) \sim \mathcal{N}(\ln(0.005^2), 0.5^2) \quad (35)$$

$$\ln(\kappa_{n+1}^2) \sim \mathcal{N}(\ln(0.1^2), 0.5^2). \quad (36)$$

Notice that these priors are not tied to the hierarchical priors for the series-specific values of these parameters, so the parameters characterizing the common factors are unrelated to those governing the series-specific factors.

In contrast, the parameters characterizing the factor loadings,  $\lambda_{j,l,t}$ , are potentially similar

across series, so that hierarchical priors are used:

$$\{\lambda_{j,0}\}_{j=1}^n \sim \mathcal{HN}(1, 0, \ln(0.2^2), 0.5^2), \quad (37)$$

$$\{\lambda_{j,l}\}_{j=1}^n \sim \mathcal{HN}(0, 0.5^2(0.05/l)^2, \ln((0.05/l)^2), 0.5^2) \text{ for } l > 0 \quad (38)$$

and

$$\{\ln(\gamma_{\lambda_{j,l}}^2)\}_{j=1}^n \sim \mathcal{HN}(\ln((0.0005/(l+1))^2), 0.5^2, \ln(0.3^2), 0.5^2). \quad (39)$$

As we mentioned at the outset of this section, the resulting complete model incorporates autoregressive dynamics, stochastic volatility, innovation and additive outliers, common factors and time-varying parameters. It uses hierarchical priors to pool information across series. The complete RTS model is given by equations (14), (17), (20), (21), (26)-(28), and (31)-(33), with priors (7)-(9), (12), (13), (15), (18), (19), (22)-(24), (29), (30), and (34)-(39).

Tables 2 and 3 and Figure 2 show the forecasting gains from the complete RTS model: the relative root-MSFEs show a 10 percent gain over the benchmark AR(12) model (Table 2), these gains are evident in nearly every state (Figure 2) and similar gains are evident in the quantile and interval forecasts (Table 3). Interestingly, additional calculations indicate that nearly all of these gains can be realized in a model in which the  $c$ -factors load only on contemporaneous values of  $u_{n+1,t}$  in (32).<sup>5</sup>

### 3.8 Bayes factors

The POOS forecast comparisons summarized in Tables 2-3 and Figure 2 show the marginal importance of the various features that appear in the RTS model, but these comparisons are lacking in two respects. First, they are based on the somewhat arbitrary sequencing of how the features appear in the models. For example, the relative importance of Student- $t$  innovations (Model III) might well change if they had been added before, rather than after, stochastic volatility (Model V). Second, the forecasting results focus on the particular aspects of accuracy associated with the loss functions from Section 2.2.2, and while these are important, they do not fully capture the overall fit of the model.

---

<sup>5</sup>We have also compared the forecasting performance of the RTS model to a dynamic version of the common correlated effects model (Pesaran (2006)) that augments the benchmark AR(12) model with 6 lags of the mean employment growth rates across the 51 states. The resulting model performed marginally better than the AR(12) model at some horizons—for example, its pooled relative root-MSFEs are (0.99, 0.98 and 0.99) for  $h = (1, 3, 6)$ —but these were markedly larger than the relative root-MSFE for the RTS model (which are (0.92, 0.89, and 0.89) for  $h = (1, 3, 6)$ ).

In this subsection we investigate the importance of the model’s features using an alternative approach: We begin with the RTS model with all features present, and compare the fit of that model to models where selected features are down-weighted. We use Bayes factors to gauge the fit of the RTS model relative to eight alternative models.

The first alternative model investigates the importance of the hierarchical priors that appear throughout the RTS model. Recall that the hierarchical normal prior assumes that a set of parameters,  $\{\theta_j\}_{j=1}^n$ , are characterized by the conditional normal prior  $\theta_j|(m_\theta, v_\theta) \sim iid\mathcal{N}(m_\theta, v_\theta)$ , where  $m_\theta$  and  $v_\theta$  are hyperparameters with their own prior distributions,  $m_\theta \sim \mathcal{N}(m_{m_\theta}, v_{m_\theta})$  and  $\ln(v_\theta) \sim \mathcal{N}(m_{\ln(v_\theta)}, v_{\ln(v_\theta)})$ ; we have denoted the resulting hierarchical prior as  $\{\theta_j\}_{j=1}^n \sim \mathcal{HN}(m_{m_\theta}, v_{m_\theta}, m_{\ln(v_\theta)}, v_{\ln(v_\theta)})$ . When  $m_\theta$  and  $v_\theta$  have degenerate distributions, that is when  $v_{m_\theta} = v_{\ln(v_\theta)} = 0$ , the prior for  $\theta_j$  collapses to the non-hierarchical normal prior  $\theta_j \sim iid\mathcal{N}(\mu_\theta, \sigma_\theta^2)$  with  $\mu_\theta = m_{m_\theta}$  and  $\ln(\sigma_\theta^2) = m_{\ln(v_\theta)}$ . (Versions of this non-hierarchical prior were used in Model I.) To gauge the importance of the hierarchical priors, it is instructive to compare the fit of the RTS model to an alternative model that uses non-hierarchical priors—that is to a model in which the hierarchical variance parameters  $v_{m_\theta}$  and  $v_{\ln(v_\theta)}$  are set to zero across all hierarchical priors. This can be achieved by computing the Bayes factor for the RTS model, with  $\{\theta_j\}_{j=1}^n \sim \mathcal{HN}(m_{m_\theta}, v_{m_\theta}, m_{\ln(v_\theta)}, v_{\ln(v_\theta)})$  relative to the model using the alternative priors  $\{\theta_j\}_{j=1}^n \sim \mathcal{HN}(m_{m_\theta}, 0, m_{\ln(v_\theta)}, 0)$ .

Unfortunately, computing Bayes factors is difficult, and we were unsuccessful in computing an accurate estimate of the Bayes factor for the RTS model versus the model with  $\{\theta_j\}_{j=1}^n \sim \mathcal{HN}(m_{m_\theta}, 0, m_{\ln(v_\theta)}, 0)$ . However, we did succeed at a less ambitious task: We accurately estimated the Bayes factor for a less extreme alternative that sets the variance of the hyperparameters equal to one-half of their values in the RTS model. (These Bayes factors were computed using the bridge sampling approach of Meng and Wong (1996) that is described in the Online Appendix.) This less-extreme alternative model attenuates, but does not eliminate, the pooling of information across series for estimating the parameter values. The resulting Bayes factor is shown in the first row of Table 4. The log-Bayes factor exceeds 80 in favor of the RTS model relative to the alternative model. Evidently, the hierarchical priors used in the RTS model more accurately describe the data than the priors in the alternative model.

Table 4 shows results for several other alternative models, where in each case these alternatives involve a change in the prior that downweights a particular feature incorporated in the RTS model.

Table 4: Log-Bayes Factors: RTS Model versus Models with Alternative Priors

Num.	RTS Model Prior	Alternative Prior	Log Bayes-Factor
(1)	$\{\theta_j\}_{j=1}^n \sim \mathcal{HN}(m_{m_\theta}, v_{m_\theta}, m_{\ln(v_\theta)}, v_{\ln(v_\theta)})$	$\{\theta_j\}_{j=1}^n \sim \mathcal{HN}(m_{m_\theta}, 0.5 \times v_{m_\theta}, m_{\ln(v_\theta)}, 0.5 \times v_{\ln(v_\theta)})$	86.1
(2)	$\{\ln(\nu_j - 2)\}_{j=1}^n \sim \mathcal{HN}(\ln(10), 0.5^2, \ln(0.5^2), 0.5^2)$	$\{\ln(\nu_j - 2)\}_{j=1}^n \sim \mathcal{HN}(\ln(10) + 1.5, 0.5^2, \ln(0.5^2), 0.5^2)$	13.8
(3)	$\{\ln(\kappa_j^2)\}_{j=1}^n \sim \mathcal{HN}(\ln(0.1^2), 0.5^2, \ln(0.3^2), 0.5^2)$	$\{\ln(\kappa_j^2)\}_{j=1}^n \sim \mathcal{HN}(\ln(0.1^2) - 1.5, 0.5^2, \ln(0.3^2), 0.5^2)$	10.9
(4)	$m_{\xi_l} \sim \mathcal{N}(0, 0.01^2)$ $\ln(v_\xi) \sim \mathcal{N}(\ln(0.01^2), 0.5^2)$	$m_{\xi_l} \sim \mathcal{N}(0, 0.5 \times 0.01^2)$ $\ln(v_\xi) \sim \mathcal{N}(\ln(0.01^2) - 1.5, 0.5^2)$	30.6
(5)	$\{\ln(\gamma_{\mu_j}^2)\}_{j=1}^n \sim \mathcal{HN}(\ln(0.005^2), 2^2, \ln(0.3^2), 0.5^2)$	$\{\ln(\gamma_{\mu_j}^2)\}_{j=1}^n \sim \mathcal{HN}(\ln(0.005^2) - 6, 2^2, \ln(0.3^2), 0.5^2)$	17.8
(6)	$\{\ln(\gamma_{\phi_{j,l}}^2)\}_{j=1}^n \sim \mathcal{HN}(\ln((0.005/l)^2), 0.5^2, \ln(0.3^2), 0.5^2)$	$\{\ln(\gamma_{\phi_{j,l}}^2)\}_{j=1}^n \sim \mathcal{HN}(\ln((0.005/l)^2) - 1.5, 0.5^2, \ln(0.3^2), 0.5^2)$	5.8
(7)	$\{\ln(\gamma_{\lambda_{j,l}}^2)\}_{j=1}^n \sim \mathcal{HN}(\ln((0.0005/(l+1))^2), 0.5^2, \ln(0.3^2), 0.5^2)$	$\{\ln(\gamma_{\lambda_{j,l}}^2)\}_{j=1}^n \sim \mathcal{HN}(\ln((0.0005/(l+1))^2) - 1.5, 0.5^2, \ln(0.3^2), 0.5^2)$	17.9
(8)	$\ln(\sigma_{n+1}^2) \sim \mathcal{N}(\ln(0.2^2), 0.5^2)$	$\ln(\sigma_{n+1}^2) \sim \mathcal{N}(\ln(0.2^2) - 1.5, 0.5^2)$	3.2

Notes: The table shows the prior used in the baseline RTS model and the prior used in the alternative model. The final column shows the log-Bayes factor of the baseline RTS model relative to the alternative. Bayes factors are computed using the 1990m2-2019m12 sample.

The second row of the table considers an alternative prior that increases the degrees-of-freedom in the Student- $t$  distribution for the innovations; that is, the prior suggests innovation distributions that are closer to the normal. The degrees of freedom parameter is denoted by  $\nu$ , and as indicated in Table 4, the alternative increases the mean of the hierarchical prior for  $\nu$ . (In the RTS model, the prior median for  $\nu$  is 12 (see (15)), while in the alternative the prior median increases to 47.) The Bayes factor reported in the table strongly favors the lower degrees of freedom in the RTS model.

The third row of the table compares the RTS model to an alternative in which the additive outliers are less important. This is achieved by using a prior with more mass on small values of  $\kappa_j$ , the scale associated with the outliers (see (17)-(18)). The Bayes factor implies that these additive outliers are quite important for describing the state employment data.

The fourth row of the table considers a model with reduced stochastic volatility. This is achieved by changing the prior to reduce the variability of the  $\xi$  parameters (see (21)-(24)); which in turn is achieved by reducing the variance of  $m_\xi$  and decreasing the mean of  $\ln(v_\xi)$ .

Again, the RTS model is strongly favored over this alternative.

The next three rows focus on time variation in the model parameters. Recall that time variation is modeled using random walk processes, and the magnitude of this time variation is governed by the variance of the associated first differences. This parameter is denoted by  $\gamma^2$  in the various equations (see (27)-(28) and (33)). We consider three alternative models, all of which are characterized by priors that lower the mean of  $\gamma^2$ . Row five of the table considers the level parameters  $\mu$ , row six considers the autoregressive coefficients  $\phi$ , and row seven considers the factor loadings  $\lambda$ . In all cases, Bayes factors suggest that time variation is important for describing the data, and this is despite the negligible impact of time variation for  $\mu$  and  $\phi$  for forecasting performance discussed above for Model VI.

The final row of the table considers an alternative in which the common factors  $c_{j,t}$  are downweighted. Recall that the  $c$ -factors are series-specific moving averages of a common autoregressive factor,  $u_{n+1,t}$ . These factors can be down-weighted by reducing the variance of  $u_{n+1}$ , that is by reducing the value of  $\sigma_{n+1}^2$  (see (34)). The final row of the table considers this alternative and here too the Bayes factor favors the prior from the RTS model, but by an amount ( $e^{3.2} \approx 25$ ) that is smaller than the other alternatives. One interpretation of this result is that common movements in the series remain well explained by the level and outlier common factors,  $\mu_{n+1}$  and  $o_{n+1}$ .

## 4 Additional empirical results

The previous sections have used the state employment dataset in the pre-COVID sample period to motivate the structure of the RTS model and to evaluate its relative forecast accuracy. In this section we investigate how the RTS model performs in other applications that involve two new datasets of related series—the growth rates of industrial production (IP) in 16 Euro-area countries and the inflation rates for 17 sectors making up personal consumption expenditures (PCE) in the United States.

### 4.1 Two new datasets

Figure 6 plots the new datasets. The top panel shows the monthly growth rates of industrial production in 16 Euro-area countries beginning in 1975m8 through 2019m12. The bottom panel shows the monthly growth rate of prices for 17 PCE sectors from 1959m2 to 2025m4. As

in the earlier application using state employment data, the Euro-area IP dataset is truncated to only include pre-COVID observations; we consider the COVID recovery period below for the employment and IP datasets. The dynamics of the inflation data over the COVID period are generally consistent with its behavior over the earlier sample period, so we analyze these data over the full sample period.

While the details differ, these datasets exhibit many of the same features as state employment. In particular they exhibit comovement, outliers, time-varying volatility, and level shifts. The series appear to follow similar stochastic processes (although inflation in one of the PCE sectors—energy—is much more volatile than the other sectors). A notable difference is that these datasets have many fewer series than the  $n = 51$  states in the employment dataset.

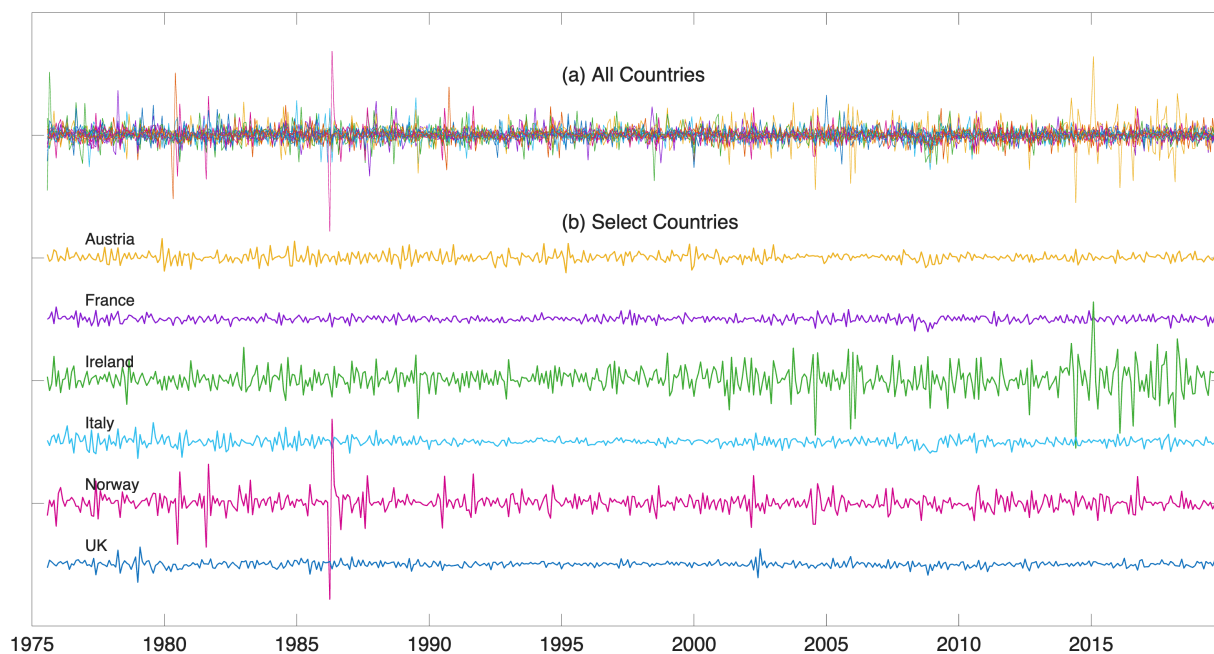
In Section 3 we developed the RTS model in seven steps and showed the forecasting performance of each of the models for the state employment data. This was a pedagogical device that allowed us to sequentially describe the various features of the model and (in the Online Appendix) the computational algorithms to accommodate these features. In this section, we skip over these preliminary models and move directly to the RTS model. We conduct the same POOS forecasting experiment used in Section 3, where the POOS forecasts are computed over 1985m6-2019m6 for the IP data and over 1984m12-2024m10 for the inflation data. The results of the experiment are summarized in Figure 7 and Table 5.

Figure 7 shows the distribution of relative root-MSFEs across the entities (states for the employment, countries for Euro-area IP, and consumption sectors for PCE inflation) for the three datasets, and where the results for state employment were shown earlier in Figure 2. Panel (a) of Table 5 shows the relative sample average values of predictive quantile and interval losses for  $h = 3$  step ahead forecasts; the values of  $h = 1$  and  $h = 6$  (not shown) are similar. Examination of these results shows that the RTS model provides forecasting gains for these new datasets that are somewhat smaller than, but broadly consistent with, the results for the state employment data.

Panel (b) of Table 5 compares the log-Bayes factors for the alternative models listed in Table 4 for the three datasets, each computed using the data through 2019m12. Here too, these Bayes factors are similar to those obtained for the state employment dataset, but with two exceptions: additive outliers are less important for the two new datasets, and the  $c$ -factor is less important for inflation. Regarding the latter, recall that the model includes three sets of common factors, level shifts ( $\mu$ ), outliers ( $o$ ) and the serially correlated  $c$ -factors. The Bayes factor for alternative model 8 only concerns the importance of the  $c$ -factor; one interpretation

Figure 6: Two Datasets

Industrial Production Growth Rates in 16 Euro Area Countries: 1975m8-2019m12



U.S. PCE Inflation in 17 Sectors: 1959m2-2025m4

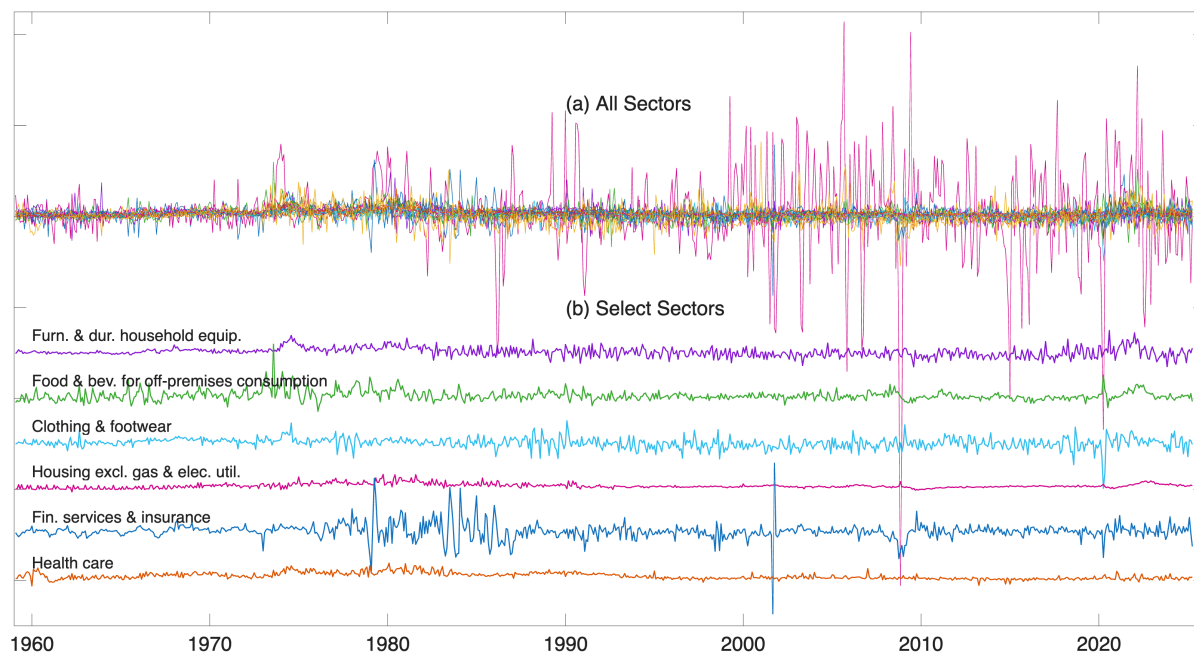
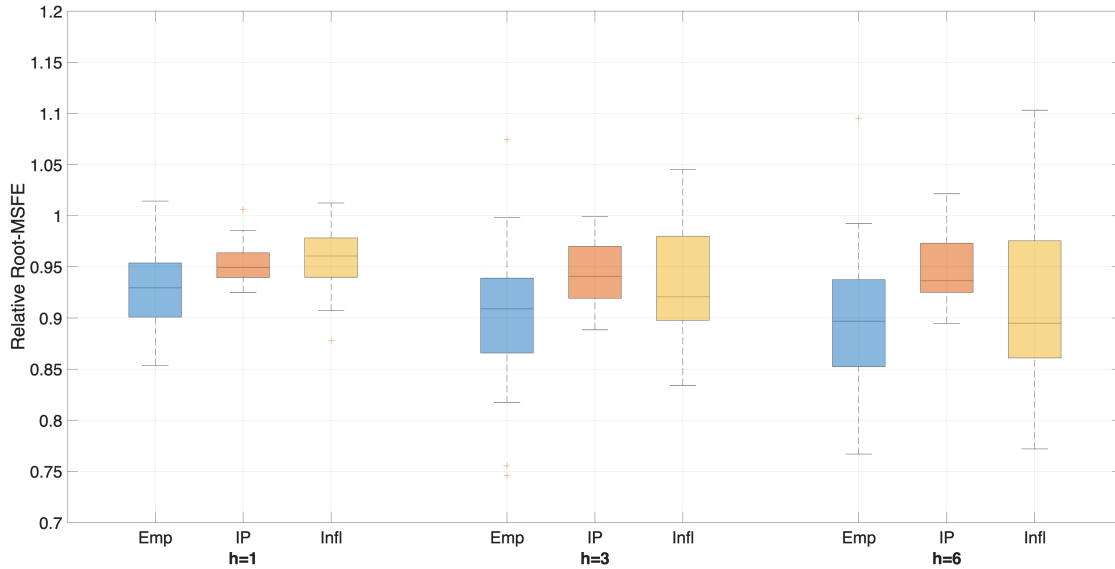


Figure 7: Relative root-MSFE for Three Datasets: Distribution Across Entities



Notes: Box plots for the relative root-MSFEs across entities the state employment (Emp), industrial production in Euro-area countries (IP), inflation in sectoral PCE (Infl) datasets for the RTS model relative to the benchmark AR(12) model.

of its value is that the common inflation trends in the sectors that are visible in Figure 6 are well described by the common level shift factor  $\mu_{n+1,t}$ .

The forecasting gains reported in Figure 7 and Table 5 are relative to the same univariate AR(12) benchmark used in Section 3. We have also compared the forecasting performance of the RTS model for inflation to a more sophisticated model, the Federal Reserve Bank of New York’s multivariate core trend inflation (MCT) model described in Almuzara and Sbordon (2022). The MCT model is a monthly extension of the quarterly model developed in Stock and Watson (2016a) for the same 17 sector decomposition of PCE inflation, and, like the RTS model, incorporates stochastic volatility, common factors and outliers. As its name suggests, the MCT model produces a monthly estimate of the “trend” in core-inflation, which can serve as a forecast of future aggregate inflation. The RTS model can also be used to forecast aggregate inflation using a share-weighted average of the sectoral inflation forecasts. Table 6 compares the relative root-MSFE of the RTS and MCT models over the 1984m12 through 2024m10 POOS sample period.<sup>6</sup> For forecasting “all-items” aggregate inflation, the MCT model is comparable to the benchmark AR(12); however, it provides substantial gains for

<sup>6</sup>We thank Martin Almuzara for sharing the MCT code, and the FRBNY for allowing us to use it for this purpose.

Table 5: Selected Results for Three Datasets

(a) Relative value of sample quantile and interval loss:  $h = 3$ 

Dataset	Quantile						90-10 Interval
	0.05	0.10	0.25	0.75	0.90	0.95	
State employment	0.83	0.85	0.88	0.91	0.89	0.87	0.87
Euro area Ind. Prod.	0.93	0.93	0.95	0.94	0.92	0.92	0.92
U.S. PCE Inflation	0.89	0.95	0.96	0.91	0.88	0.86	0.91

(b) Log-Bayes Factors

Dataset	Alternative Model							
	1	2	3	4	5	6	7	8
State employment	86.1	13.8	10.9	30.6	17.8	5.8	17.9	3.2
Euro area Ind. Prod.	43.5	10.8	0.0	23.4	8.2	5.9	3.7	5.7
U.S. PCE Inflation	76.8	9.8	-0.4	33.9	11.7	28.8	0.9	-1.3

Notes: Panel (a): Relative values of pooled sample quantile and interval risk. Panel (b): log-Bayes factors for the RTS model versus the 8 alternative models listed in Table 4.

Table 6: Relative root-MSFE for Aggregate Inflation

Forecasting Model	All items			Core (excl. Food and Energy)		
	$h = 1$	$h = 3$	$h = 6$	$h = 1$	$h = 3$	$h = 6$
RTS Model	0.98	0.95	0.92	0.93	0.88	0.83
FRBNY-MCT	1.03	0.99	1.00	0.96	0.90	0.86

Notes: The table reports the root-MSFE relative to the sector-specific benchmark AR(12) model, where the forecast of aggregate inflation is the share-weighted average of the sectoral forecasts over the 1984m12-2024m10 POOS sample period.

core inflation—that is, for aggregate inflation excluding the volatile food and energy sectors. The RTS model provides improvements for both all-items and core-inflation relative to both the benchmark AR(12) model and the MCT forecasts.<sup>7</sup>

## 4.2 Forecasting during the COVID recovery

The COVID-19 pandemic led to dramatic declines in employment and economic activity in the first half of 2020 and the subsequent recovery involved dynamics that differed from the

<sup>7</sup>We have also compared the forecasting performance of the RTS model to a version of the “random-walk” model used in Atkeson and Ohanian (2001); that paper considered quarterly data on inflation and used average inflation over the past four quarters to predict the average value of inflation over the next four quarters. Here we use average inflation over the last twelve months to predict average inflation over the next  $h$  months, with  $h = 1, 3, 6$ . Pooled root-MSFE for the RTS forecasts relative to the AO forecasts for  $h = 1, 3, 6$  are (0.90, 0.88, 0.80). The corresponding values for all-items aggregate inflation are (0.90, 0.90, 0.87), and for core aggregate inflation they are (0.98, 0.95, 0.93).

pre-COVID period.<sup>8</sup> Both of these features are evident in Figure 8, which plots the state employment growth rates over 2017m1-2025m4 in panel (a) and the growth rate of Euro-area industrial production (IP) over 2017m1-2023m10 in panel (b). (The IP data is only available for this truncated sample.) Additionally, panel (b) shows one country—Ireland—with a marked increase in volatility and/or outliers during the post-COVID period. Needless to say, forecasting during the COVID recession and its aftermath was challenging.

Time series (and other) models were ill-equipped to forecast the dramatic changes in employment that occurred during the first half of 2020, and we will continue to omit this period from our POOS forecasting experiment. A more interesting question is how well models performed in the aftermath of the COVID recession. For example, because  $AR(p)$  models rely on lags, the outliers in early 2020 continue to affect the AR model forecasts  $p$  periods after the COVID outliers. The RTS model, with its allowance for outliers, stochastic volatility and time-varying coefficients, can more easily downweight these outliers and adapt to changes in the economy’s dynamics. Thus, one expects that the RTS model will perform better than the  $AR(12)$  model following COVID. But how much better, and how quickly will these relative gains dissipate as the economy returns to its pre-COVID dynamics?

Table 7 reports results from the POOS experiment to answer these questions. In particular, it shows the root-MSFE pooled across the 51 states (panel (a)) and the 16 Euro-area countries for the benchmark  $AR(12)$  model over three POOS periods: pre-COVID and two post-COVID periods, the first beginning in 2020m6 and the second in 2021m6. It also shows the relative root-MSFE of the RTS model over these sample periods and relative sample loss for the 90-10 prediction interval.

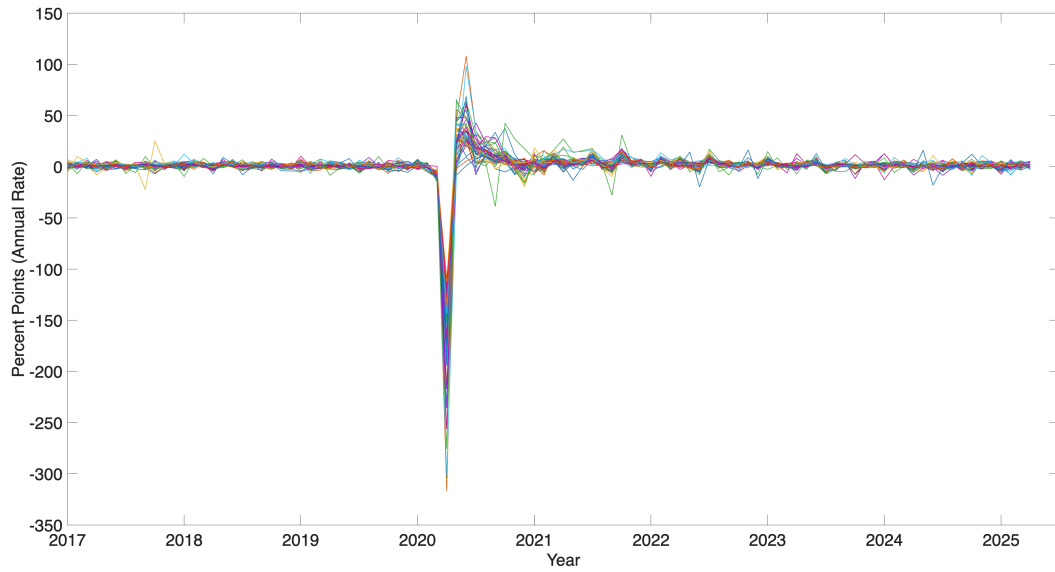
Looking first at the results for the state employment in panel (a), the pre-COVID period results were shown previously: for example the benchmark  $AR(12)$  model has a root-MSFE of 2.1 percentage points for  $h = 3$ ; the RTS model’s root-MSFE is 11 percent lower. For the forecasts beginning in 2020m6, the root-MSFE for the  $AR(12)$  increases sharply to 16.5 percentage points; the RTS model’s increases too, but only to 3.5 percentage points. For forecasts beginning in 2021m6, the  $AR(12)$  model is not directly affected by the COVID outliers and its forecasting performance returns to levels similar to the pre-COVID period. The RTS model performance also improves during this period, so much so that its relative root-MSFE is below its pre-COVID value.

---

<sup>8</sup>See Stock and Watson (2025) for an empirical analysis of the dynamics of real activity in the U.S. in the recovery from the COVID recession.

Figure 8: State Employment and Euro-area IP Growth Rates During COVID

(a) State Employment Growth Rates, 2017m1-2025m4



(b) Euro-Area IP Growth Rates, 2017m1-2023m10

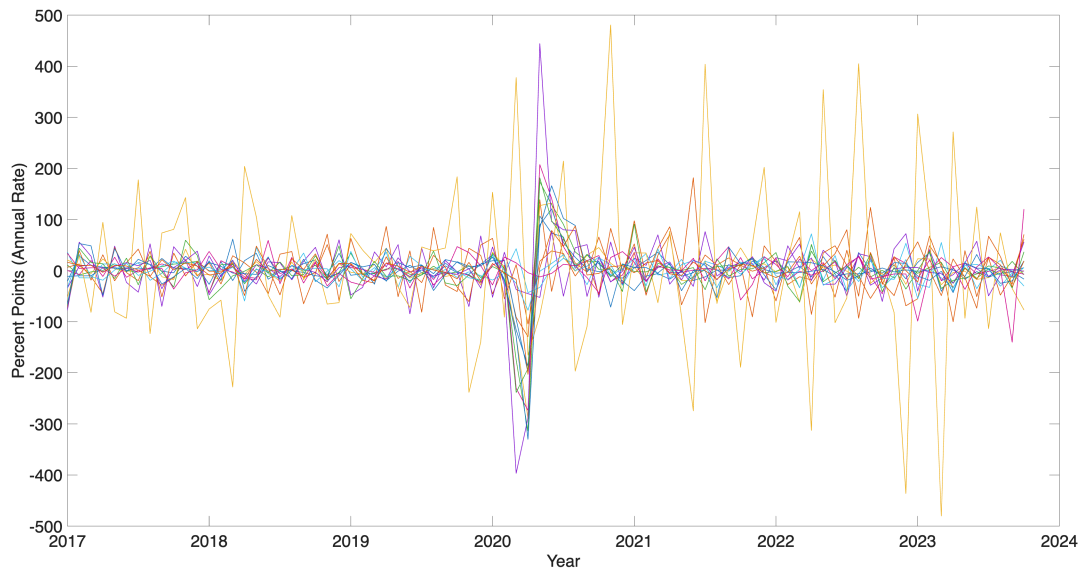


Table 7: Root-MSFE and Forecast 90-10 Interval Risk in Pre- and Post-COVID Sample Periods

POOS forecast period	h = 1				h = 3				h = 6		
	AR root-MSFE	RTS relative MSFE	RTS relative 90-10 Interval		AR root-MSFE	RTS relative MSFE	RTS relative 90-10 Interval		AR root-MSFE	RTS relative MSFE	RTS relative 90-10 Interval
	(a) State Employment										
1999m12-2019m6	3.3	0.92	0.90		2.1	0.89	0.87		1.8	0.89	0.86
2020m6-2024m10	26.4	0.21	0.20		16.5	0.21	0.18		7.8	0.29	0.27
2021m6-2024m10	4.2	0.88	0.50		2.4	0.74	0.43		1.8	0.69	0.47
	(b) Euro-Area Industrial Production										
1985m6-2019m6	31.7	0.96	0.92		13.2	0.96	0.92		8.4	0.95	0.94
2020m6-2023m4	62.8	0.97	0.82		27.6	0.81	0.63		14.9	0.88	0.73
2021m6-2023m4	54.0	1.0	0.88		20.6	0.97	0.80		12.3	1.00	0.85

Notes: The entries are absolute root-MSFE of the AR(12) benchmark model, as well as the relative root-MSFE and relative interval risk of the RTS model over three sample periods.

The results for Euro-area industrial production are less dramatic. The fall and recovery of Euro-area industrial production during COVID was much smaller than for U.S. employment. The benchmark AR(12) root-MSFE for the period beginning in 2020m6 is roughly twice as large as its pre-COVID value, versus nearly eight times larger for the state employment data, and the relative gains from using the RTS, while greater in the immediate aftermath of COVID, are not as large as those for the U.S. employment data.

Overall, we are reassured by these external validity tests: the RTS performs reasonably well for two additional data sets and it adapts well to the dramatic changes in the economy associated with the COVID pandemic.

## 5 Concluding remarks

This paper has developed a model for forecasting “related” time series. The resulting RTS model exploits similarity in the stochastic processes describing the individual series as well as covariation between the series. The paper also developed MCMC methods to efficiently obtain draws from the posterior distribution of the model’s parameters and predictive distributions. Modeling and computation go hand-in-hand in forecasting applications such as this—a model is useful only to the extent that it can be implemented.

The RTS model was developed to capture features in macro datasets such as the state employment, Euro-area industrial production and sectoral inflation data analyzed in the paper. The variables in these datasets are, to first order, well described by simple univariate

autoregressions with similar coefficient values, but additionally exhibited stochastic volatility, heavy-tailed innovations, occasional large outliers, common sources of variability, and slowly drifting parameters. The RTS model incorporates all of these features.

In other applications, researchers may want to include all or only a subset of these features. The modular design of the MCMC algorithms described in the Online Appendix makes them well-suited for such applications.

## References

- ABRAHAM, B., AND G. E. BOX (1979): “Bayesian Analysis of Some Outlier Problems in Time Series,” *Biometrika*, 66(2), 229–236.
- ALMUZARA, M., AND A. SBORDONE (2022): “Inflation Persistence: How Much is There and Where Is It Coming From?,” *Federal Reserve Bank of New York Liberty Street Economics*, <https://libertystreeteconomics.newyorkfed.org/2022/04/inflation-persistence-how-much-is-there-and-where-is-it-coming-from/>.
- ANTOLIN-DIAZ, J., T. DRECHSEL, AND I. PETRELLA (2024): “Advances in Nowcasting Economic Activity: The Role of Heterogeneous Dynamics and Fat Tails,” *Journal of Econometrics*, 238, Article 105634.
- ATKESON, A., AND L. E. OHANIAN (2001): “Are Phillips Curves Useful for Forecasting Inflation?,” *Federal Reserve Bank of Minneapolis Quarterly Review*, 25(1), 2–11.
- BAI, Y., A. CARRIERO, T. CLARK, AND M. MARCELLINO (2022): “Macroeconomic Forecasting in a Multi-Country Context,” *Journal of Applied Econometrics*, 37(6), 1230–1255.
- BANBURA, M., D. GIANNONE, AND L. REICHLIN (2010): “Large Bayesian Vector Autoregressions,” *Journal of Applied Econometrics*, 25(1), 71–92.
- BOX, G. E. P., AND G. M. JENKINS (1970): *Time Series Analysis: Forecasting and Control*. Holden-Day, San Francisco.
- CARRIERO, A., T. E. CLARK, AND M. MARCELLINO (2015): “Bayesian VARs: Specification Choices and Forecast Accuracy,” *Journal of Applied Econometrics*, 30(1), 46–73.
- CARRIERO, A., T. E. CLARK, M. MARCELLINO, AND E. MERTENS (2024): “Addressing Covid-19 Outliers in BVARs with Stochastic Volatility,” *Review of Economics and*

- Statistics*, 106(5), 1403–1417.
- CHAN, J., AND I. JELIAZKOV (2009): “Efficient Simulation and Integrated Likelihood Estimation in State Space Models,” *International Journal of Mathematical Modeling and Numerical Optimization*, 1, 101–120.
- CHUDIK, A., AND M. H. PESARAN (2016): “Theory and Practice of GVAR Modeling,” *Journal of Economic Surveys*, 30(1), 165–197.
- COGLEY, T., AND T. J. SARGENT (2005): “Drifts and Volatilities: Monetary Policies and Outcomes in the Post WWII US,” *Review of Economic Dynamics*, 8, 262–302.
- D’AGOSTINO, A., AND D. GIANNONE (2012): “Comparing Alternative Predictors Based on Large-Panel Factor Models,” *Oxford Bulletin of Economics and Statistics*, 74(2), 306–326.
- DE MOL, C., D. GIANNONE, AND L. REICHLIN (in press): “The Asymptotic Equivalence of Ridge and Principal Component Regression with Many Predictors,” *Econometrics and Statistics*.
- DEL NEGRO, M., AND C. OTROK (2008): “Dynamic Factor Models with Time-Varying Parameters: Changes in International Business Cycles,” *Federal Reserve Bank of New York, Staff Report 326*.
- DOAN, T., R. LITTERMAN, AND C. SIMS (1984): “Forecasting and Conditional Projection Using Realistic Prior Distributions,” *Econometric Reviews*, 3, 1–100.
- DURBIN, J., AND S. J. KOOPMAN (2002): “A Simple and Efficient Simulation Smoother for State Space Time Series Analysis,” *Biometrika*, 89(3), 603–615.
- ENGLE, R. F. (1982): “Autoregressive Conditional Heteroscedasticity with Estimates of the Variance of United Kingdom Inflation,” *Econometrica*, 4, 987–1007.
- FOX, A. (1972): “Outliers in Time Series,” *Journal of the Royal Statistical Society, Series B*, 34(3), 350–363.
- GELMAN, A., J. B. CARLIN, H. S. STERN, AND D. B. RUBIN (2004): *Bayesian Data Analysis*. Chapman & Hall/CRC, Boca Raton, Florida, 2nd edn.
- GEWEKE, J. (2004): “Getting It Right: Joint Distribution Tests of Posterior Simulators,” *Journal of the American Statistical Association*, 99, 799–804.

- HARVEY, A. C. (1989): *Forecasting, Structural Time Series Models and the Kalman Filter*. Cambridge University Press.
- HENDRY, D. F., AND K. HUBRICH (2011): “Combining Disaggregate Forecasts or Combining Disaggregate Information to Forecast and Aggregate,” *Journal of Business and Economic Statistics*, 29(2), 216–227.
- KIM, S., N. SHEPHARD, AND S. CHIB (1998): “Stochastic Volatility: Likelihood Inference and Comparison with ARCH Models,” *Review of Economic Studies*, 65, 361–393.
- MENG, X. L., AND W. H. WONG (1996): “Simulating Ratios of Normalizing Constants via a Simple Identity: a Theoretical Exploration,” *Statistica Sinica*, 6, 831–860.
- NERLOVE, M., D. GREETHER, AND J. CARVALHO (1979): *Analysis of Economic Time Series*. Academic Press.
- NYBLÖM, J. (1989): “Testing for the Constancy of Parameters Over Time,” *Journal of the American Statistical Association*, 84, 223–230.
- OMORI, Y., S. CHIB, N. SHEPHARD, AND J. NAKAJIMA (2007): “Stochastic Volatility with Leverage: Fast and Efficient Likelihood Inference,” *Journal of Econometrics*, 140, 425–449.
- PESARAN, M. H. (2006): “Estimation and Inference in Large Heterogeneous Panels with Multifactor Error Structure,” *Econometrica*, 74, 967–1012.
- STOCK, J. H., AND M. W. WATSON (2016a): “Core Inflation and Trend Inflation,” *Review of Economics and Statistics*, 98(4), 770–784.
- (2016b): “Factor Models and Structural Vector Autoregressions in Macroeconomics,” in *Handbook of Macroeconomics*, ed. by J. B. Taylor, and H. Uhlig, vol. 2A, pp. 415–526. North Holland.
- (2025): “Recovering From Covid,” *Brookings Papers on Economic Activity*, Spring, 2025.